


Continuous extrusion foaming process of biodegradable nanocomposites based on poly(lactic acid)/carbonaceous nanoparticles with different geometric shapes: An insight into involved physical, chemical and rheological phenomena

Amirali Soleimanpour¹ | Hanieh Khonakdar¹ | Seyed Rasoul Mousavi² |
 Nastaran Banaei¹ | Farkhondeh Hemmati³ | Mohammad Arjmand² |
 Holger Ruckdäschel⁴  | Hossein Ali Khonakdar^{1,4}

¹Department of Polymer Processing, Iran Polymer and Petrochemical Institute, Tehran, Iran

²Nanomaterials and Polymer Nanocomposites Laboratory, School of Engineering, University of British Columbia, Kelowna, British Columbia, Canada

³Caspian Faculty of Engineering, College of Engineering, University of Tehran, Guilan, Iran

⁴Department of Polymer Engineering, University of Bayreuth, Bayreuth, Germany

Correspondence

Dr. Farkhondeh Hemmati, Caspian Faculty of Engineering, College of Engineering, University of Tehran, Guilan, Iran.

Email: f.hemmati@ut.ac.ir and Hossein Ali Khonakdar, Department of Polymer Processing, Iran Polymer and Petrochemical Institute, Tehran, Iran. Email: h.khonakdar@ippi.ac.ir

Abstract

One-step extrusion foaming process of biodegradable poly(lactic acid) (PLA)-based nanocomposites in the presence of chemical foaming agent and chain extender has great complexity to control. In this work, PLA-based nanocomposites containing different carbonaceous nanoparticles with different geometric shapes were obtained through a co-rotating twin-screw extrusion process to get insight into the dominant phenomena, which control the structural and final properties of PLA foams. The reactive extrusion foaming of PLA melt was investigated in the presence of carbon black, carbon nanotubes (CNTs), graphene oxide (GO), and a chain extender additive as well as a chemical foaming agent. Nanoparticles affect the continuous extrusion foaming of PLA melt through several phenomena, including providing bubble heterogeneous nucleation sites, intensifying the chemical decomposition of the foaming agent, improving the PLA structural modification reaction, increasing PLA molecular weight and restricting the dissolved gas removal from the melt. By influencing the involved phenomena in process, the nanoparticles at low levels, especially CNT and GO, increased the void content and cell size of PLA foams. The incorporation of CNT and GO nanofillers at the 0.5 phr level increased the electrical conductivity of PLA foams sharply by 9 and 10 orders of magnitude, resulting in lightweight, biodegradable semi-conductive foams.

KEYWORDS

carbonaceous nanoparticles, electrical conductivity, molecular weight, morphology, poly(lactic acid) foam, rheological behavior

This is an open access article under the terms of the [Creative Commons Attribution](https://creativecommons.org/licenses/by/4.0/) License, which permits use, distribution and reproduction in any medium, provided the original work is properly cited.

© 2023 The Authors. *Journal of Applied Polymer Science* published by Wiley Periodicals LLC.

1 | INTRODUCTION

State-of-the-art polymers are of the advantageous materials today. Extremely used in a wide range of applications, advanced polymers will be among the undeniable materials in the upcoming years. Revolutionize in biomedical devices, spacecraft, fuel consumption, etc., is no longer inaccessible with improving the polymer industry.^{1–4} Recently, many attempts have been made to replace fossil fuel-based synthetic polymers with biodegradable and biocompatible polymers because of concerns regarding environmental issues.^{5–8} Poly(lactic acid) (PLA) is a renewable polymer made from potato, bagasse, sugarcane, corn, wheat, and rice.^{9–13} PLA exhibits exceptional biocompatibility and hydrolysis ability. Also, it emissions no toxic gases during the synthesis process. This is why PLA has drawn much attention for applications such as drug release and tissue engineering. Besides, because of the satisfactory processability of PLA, it can be used in the packaging industry.^{14–16} PLA foams can be replaced with ordinary foams in packaging applications because of the cost-effective production process, suitable mechanical properties, superior biodegradability, and so on.^{17–21}

Notwithstanding the merits of PLA foams, they have some demerits, such as low operating temperatures, slow crystallization kinetics, and low melt strength, which require overcoming to allow their commercialization. The poor melt strength of PLA plays a negative role in cell growth and mostly leads to cell wall rupture.^{22,23} To overcome the mentioned drawbacks, different modification techniques, including nanoparticle incorporation,²⁴ crosslinking,²⁵ copolymerization,²⁶ chain extension,²⁷ and producing PLA/polymer blends,²⁸ have been performed. Crosslinking would led to some unfavorable influence such as producing gel, and also deteriorating the biodegradability nature of PLA.²⁶ In the case of chain extenders (CEs), in the molten state, the reaction between CEs and the OH or COOH presented in PLA chains leads to converting the linear ones to long-chain molecules with greater melt strength and molecular weight.²⁹ In the case of producing PLA/polymer blends, reactive compatibilizers have been extensively used for improving the low interfacial adhesion of polymer phases and controlling the dispersion state, bringing in various chain segments to PLA.³⁰

Many studies have been dedicated to use of CEs and nanoparticles in the foaming process of PLA. For instance, in the work of Keshtkar et al.³¹ incorporating dissolved CO₂ and various percentages of nanoclay in the PLA were studied. The outcomes indicated that the

PLA crystallization kinetics was extremely enhanced. In addition, cell density and expansion ratio highly increased as clay content was increased. In another work, Guan et al.³² added chitin nanowhiskers (CNW) to pure PLA and PLA/polyhydroxybutyrate-valerate (PHBV) blend foams. They investigated the physical and mechanical behavior of the produced foams. As their outcomes suggested, incorporating small loadings of CNW increased the mechanical behavior of unfoamed blends. Also, the strength and expandability of foamed blends filled with CNW extremely enhanced compared to those of virgin blend foams.

Type and geometric shape of nanofillers significantly affect the performance of the final foam as well as the phenomena during extrusion foaming process. For example, graphene improves Young's modulus and viscosity, and, carbon nanotubes lead to an improvement in foam morphology and melt strength.^{33,34} Herein, we have attempted to improve the PLA foamability with the incorporation of chain extender and carbonaceous nanofillers. To better understand the phenomena involved in the extrusion process, which control the foam morphology and density, molecular weight and rheological behavior have been also studied. Although biodegradable PLA thermoplastic foam has the potential to replace the commercial foams based on synthetic thermoplastics like polystyrene, the foamability of PLA melt in industrial foaming processes like extrusion needs to be improved. The main objective of this work is to enhance the foaming ability of PLA melt by adding different carbonaceous nanofillers and chain extender in continuous extrusion foaming process to expand the potential applications of semi-conductive PLA foams.

2 | EXPERIMENTAL PROCEDURE

2.1 | Materials

Poly (L-lactic acid) (PLA), grade 2003D, was supplied by Nature Works LLC, USA. Long multi-walled carbon nanotubes (CNT) and graphene oxide (GO) were obtained from Sigma Aldrich, USA. CB (N330) was purchased from Pars Carbon Black, Iran. The polymeric CE, Joncryl ADR[®] 4400, was prepared from BASF (Ludwigshafen, Germany). Moreover, as the chemical foaming agent, azodicarbonamide (AzD, 7000 dB) was purchased from Kum Yang, South Korea. In addition, zinc oxide, as the chemical foaming agent activator, was prepared from Merck, Germany. Table 1 indicates the physical properties of used materials.

TABLE 1 Physical properties of the used materials.

Material	Property	
PLA	Specific gravity	1.24
	MFI (g/10 min)	6
CNT	Diameter (nm)	110–170
	Length (μm)	5–9
	Surface area (m ² /g)	1.3 × 10 ²
GO	Sheets	15–20
	Edge oxidized (%)	4–10
CE	EEW (g/mol)	485
	Average molecular weight (g/mol)	7100

Abbreviations: EEW, epoxy equivalent weight; MFI, melt flow index.

2.2 | Sample preparation

2.2.1 | Un-foamed samples

Firstly, the raw materials were dried in a vacuum oven at 60°C for 12 h. Then, PLA, and different contents (0.25, 0.5, and 1 phr) of CB, CNT, and GO were mixed via a two-screw extruder (Rondol micro compounder, UK) at 150 rpm. The temperature profile (hopper to die) was selected to be 140°C, 145°C, 160°C, 160°C, and 160°C. Afterward, a pelletizing machine was used to pelletize the materials.

2.2.2 | Foamed samples

First, the raw materials were dried in a vacuum oven at 60°C for 12 h. Then, PLA, different contents (0.25, 0.5, and 1 phr) of CB, CNT, and GO, and constant amounts of AzD (4 phr), zinc oxide (0.25 phr), and CE (5 phr) were mixed via the same extruder at 150 rpm. The temperature profile (hopper to die) was selected to be 140°C, 145°C, 160°C, 160°C, and 160°C. Herein, the samples were expressed as “X-PLA/YZ,” where X represents whether the sample is foamed or un-foamed (f or uf, respectively), Y indicates the nanoparticle content, and Z denotes the nanoparticle type. For instance, the foam filled with 0.25 phr CNT was expressed as “f-PLA/0.25CNT.” It is noteworthy that the f-PLA control sample was also prepared using the same processing conditions. This foam contains fixed amounts of AzD (4 phr), zinc oxide (0.25 phr), and CE (5 phr), though without any nanofillers. Our experiments showed that virgin PLA without CE additive could not be foamed at the extrusion process under the same processing conditions. Melt drooling, disintegration in addition to intense bubble wall rupture

and gas removal from melt were observed in the extrusion foaming of virgin PLA after exiting the extruder die. Therefore, f-PLA foam with CE additive was used as a control sample.

2.3 | Characterizations

2.3.1 | Void content

ASTM D 1622 was used to determine the foams' density. In addition, ASTM D 792 was utilized to calculate the un-foamed samples' density using the solvent displacement procedure. The solvent in this study was normal hexane (density = 0.66 g/cm³). Moreover, the void content was determined following ASTM D 2734 via the below relation:

$$V_f = \frac{d_{uf} - d_f}{d_{uf}} \times 100, \quad (1)$$

where, V_f denotes the cavity fraction, and d_{uf} and d_f are the density of un-foamed and foamed samples, respectively.

2.3.2 | Morphological studies

The samples were cryogenically fractured, and the morphology studies were carried out on their surfaces via a Vegall Tescan scanning electron microscope (SEM). The following equations were used to calculate the number-average diameter of bubbles (D_n), the volume-average diameter of bubbles (D_v), and cell density (N_c).

$$D_n = \frac{\sum(n_i d_i)}{\sum n_i}, \quad (2)$$

$$D_v = \frac{\sum(v_i d_i)}{\sum v_i}, \quad (3)$$

$$N_c = \left(\frac{n}{A}\right)^{1.5 (d_{un}/d_f)}, \quad (4)$$

where n and d are the cell number and diameter, respectively. Also, A is the surface area of foamed sample.

To investigate the dispersion state of nanofillers in the PLA matrix, the un-foamed samples were cut into 100 nm thick slices with a cryo-microtome device, and

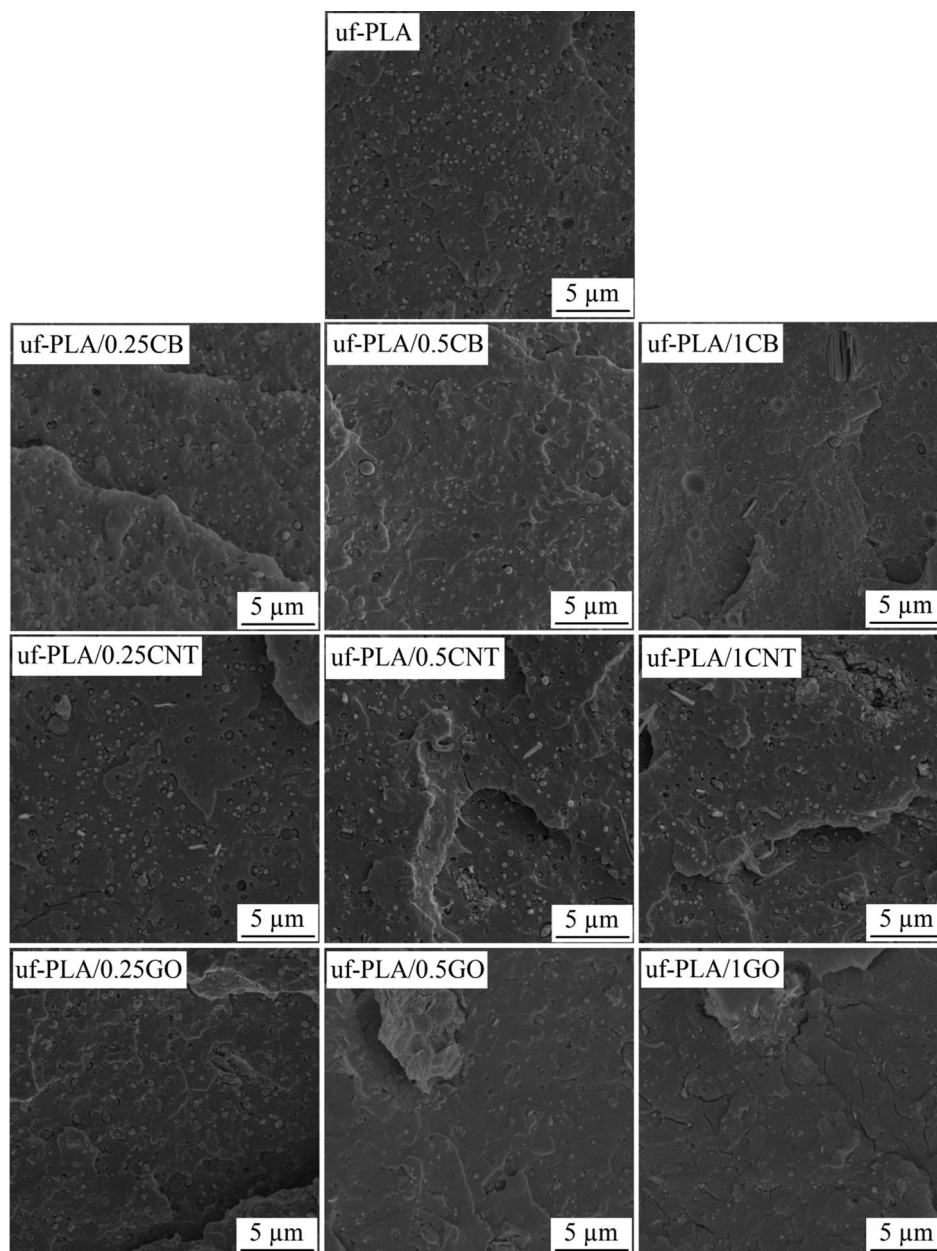


FIGURE 1 SEM images of the cryo-fractured surfaces of un-foamed samples.

afterward, they were observed via a transmission electron microscope (TEM; libra200).

2.3.3 | Rheometric mechanical spectroscopy (RMS)

The melt linear viscoelastic behavior of the foams was investigated via RMS. The oscillatory shear measurements (frequency sweep test) were performed at 170°C, a linear strain of 1%, and under an N₂ environment via an Anton Paar parallel plate rheometer (MCR30, Austria) equipped with parallel plate geometry in which the diameter and gap were 25 and 1 mm, respectively.

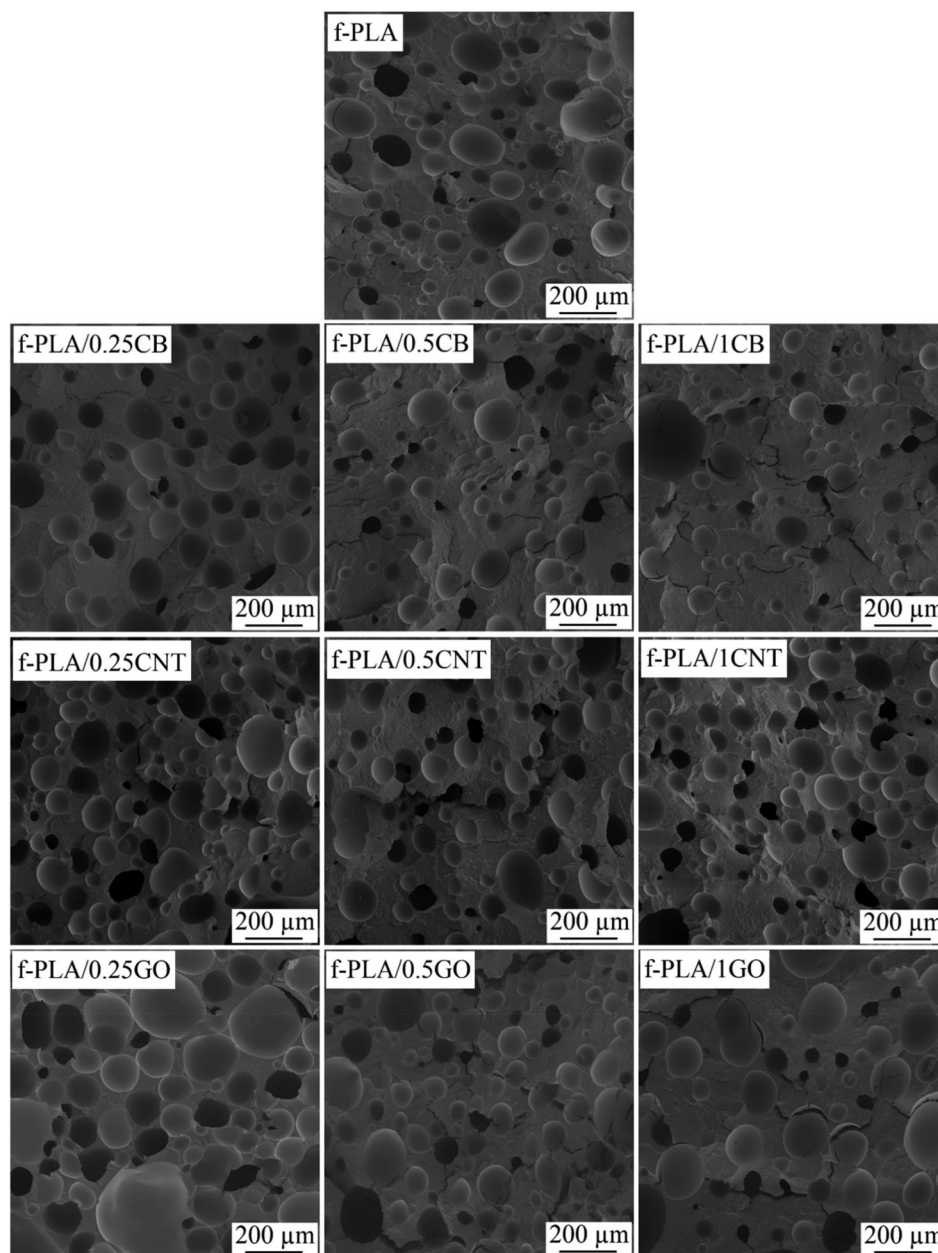
2.3.4 | Gel permeation chromatography (GPC)

The number- and weight-average molecular weights (\overline{M}_n and \overline{M}_w , respectively) of PLA chains and Polydispersity Index (PDI) in the presence of carbonaceous nanoparticles were determined via GPC (Agilent, USA) after dissolving the foams in tetrahydrofuran solvent.

2.3.5 | Electrical conductivity

Volume electrical conductivity test was conducted on the foamed samples with the dimensions of 100 × 100

FIGURE 2 SEM images of foamed samples.



$\times 1 \text{ mm}^3$ using a microcurrent detector (EST121, Hua Jing Hui Tech, China) under a voltage of 500 V, according to the GB/T 1410-2006 standard.

3 | RESULTS AND DISCUSSIONS

3.1 | Scanning electron microscopy

3.1.1 | Un-foamed samples

As can be observed in Figure 1, the un-foamed PLA (uf-PLA) cryo-fractured surface is smooth and glassy, revealing its brittle nature. Adding nanofillers in uf-PLA led to non-uniform surfaces regardless of the nanofiller type.

Surfaces with less uniformity can be observed at higher nanofiller loading.³⁵ Moreover, the loading of low carbon nanofillers did not lead to aggregation, but the greater the nanoparticles content, the higher the nanofillers aggregations and the surface roughness. These observations reveal the appropriate compounding process.³⁶

3.1.2 | Foamed samples

The SEM images of foamed samples are shown in Figure 2. Also, V_f , N_c , D_v , and D_n , determined from SEM micrographs for all foamed samples, are gathered in Figure 3. It was observed that the presence of nanofillers influences the morphology of foamed PLA (f-PLA)

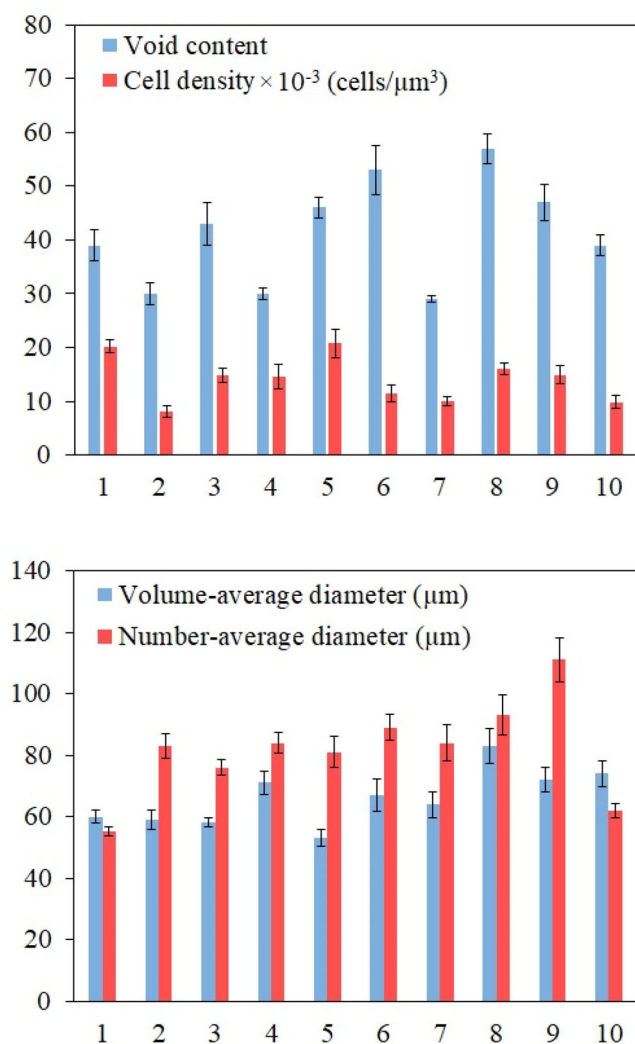


FIGURE 3 The data obtained from SEM images for (1) f-PLA, (2) f-PLA/0.25CB, (3) f-PLA/0.5CB, (4) f-PLA/1CB, (5) f-PLA/0.25CNT, (6) f-PLA/0.5CNT, (7) f-PLA/1CNT, (8) f-PLA/0.25GO, (9) f-PLA/0.5GO, and (10) f-PLA/1GO. [Color figure can be viewed at wileyonlinelibrary.com]

regardless of the carbonaceous nanoparticles type. In addition, the degree of sphericity, size, and homogeneity of cells were altered by adding nanofillers to f-PLA.

For the f-PLA samples loaded with different percentages of CB, the void content of the foam containing 0.5 phr CB was enhanced by about 10%, while its cell density dropped by almost 27%. In the case of f-PLA samples containing CNT, although the void content of f-PLA/0.25CNT and f-PLA/0.5CNT improved by approximately 18% and 36%, respectively, different trends were seen for their cell density. The cell density of f-PLA/0.25CNT enhanced by around 3%, whereas that of f-PLA/0.5CNT decreased by approximately 43%. For f-PLA/GO samples, the void contents of all samples experienced an improvement or no alteration than f-PLA. Moreover, the

cell density of all samples diminished. The most significant increment in void content (46%) was seen for the foam containing 0.25 phr of GO, whereas its cell density experienced a diminishment by almost 21%.

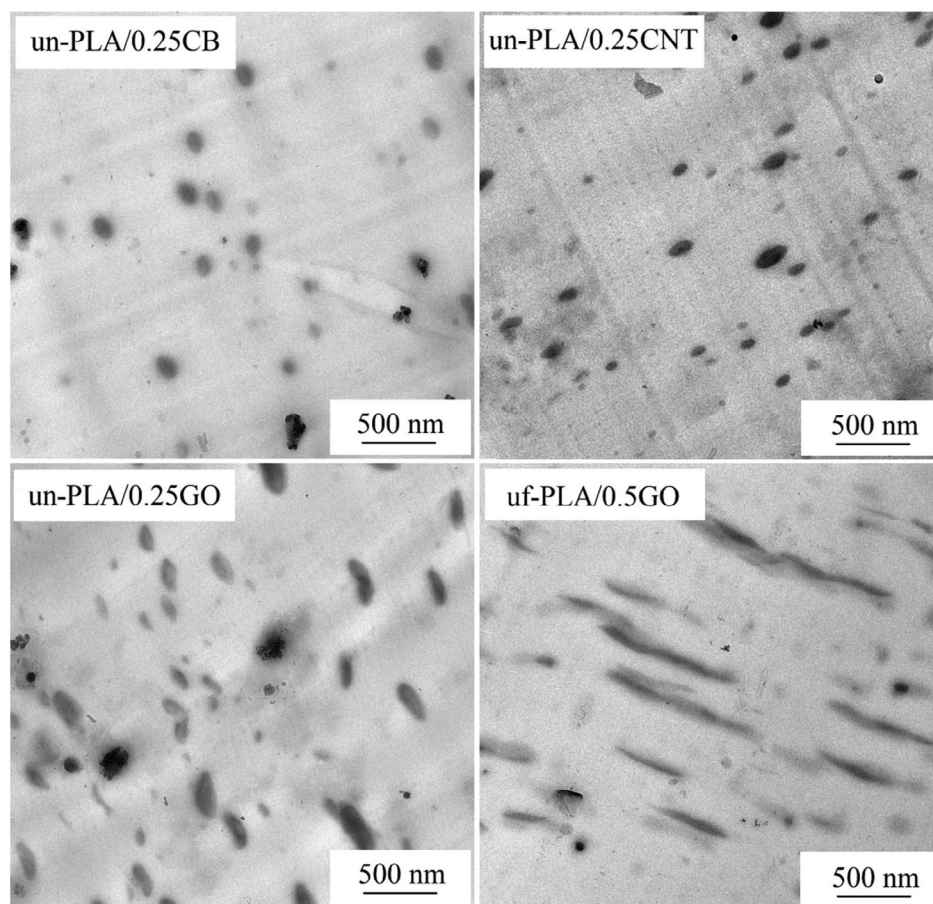
Additionally, it should be noted that regardless of the nanofillers type, the void content and cell density of f-PLA loaded with 1 phr nanofiller diminished in comparison with either those of neat f-PLA or f-PLA with 0.25 and 0.5 phr carbonaceous nanofillers. The reason for this may be the nanofillers aggregation after adding 1 phr of each. Besides, it is worth mentioning that due to the low viscosity of PLA melt, caused by chain scission and carbonaceous nanofillers incorporation, the shear flow field during mixing is not enough for gas to be diffused adequately, hence producing more homogeneous polymer-gas mixture. Additionally, the presence of nanoparticles, especially GO nanoplatelets, can provide a barrier against the removal of gas obtained from the foaming agent decomposition. Consequently, the void content of nanocomposites and average cell size at lower loadings of nanofillers are improved comparing with the ones for virgin PLA.

Moreover, the foam loaded with 0.25 phr CNT has the maximum cell density. Besides, the maximum void content and the minimum standard deviation belong to the foam containing 0.25 phr GO, suggesting its cells homogeneity. This is because of homogeneous cell nucleation without external nuclei and poor melt strength.³⁷ Among different used nanofillers, CNT nanoparticles have provided the largest heterogeneous nucleation sites for bubbles, leading to the largest cell density and the most uniform cells.

The number-average diameters of bubbles in all prepared nanocomposites are all larger than the D_n of f-PLA foam. It seems that the nanofiller loading has negligible effect on D_n , except for nanocomposite foams containing GO nanoparticles. At 1 phr loading of GO, the beneficial influence of the nanofiller on the foamability of PLA is weakened owing to dispersion and delamination state of GO nanoplatelets. A similar trend can be observed for the volume-average cell diameter in the presence of nanofillers. For almost all prepared nanocomposite foams, D_V is larger than that of f-PLA sample. Just f-PLA/0.25CNT shows smaller D_V than f-PLA foam. As mentioned earlier, the reason for its acceptability is the better nucleation effect of CNT nanoparticles for bubbles.

Accordingly, the explanations mentioned above reveal that the most optimum properties can be observed in the foams loaded with 0.25 phr CNT and 0.25 phr GO. The foam filled with 0.25 phr GO has the largest increase in void content ($\sim +45\%$) than neat foam, whereas the cell density of this sample diminishes by approximately 20%. In addition, notwithstanding less

FIGURE 4 TEM images of un-foamed nanocomposite samples.



increment in void content (+18%), the foam filled with 0.25 phr CNT indicates a + 3% increment in cell density than pure foam.

3.2 | Transmission electron microscopy

The TEM images of un-foamed nanocomposites can be observed in Figure 4. It can be seen that the nanofillers are well dispersed in uf-PLA, and no apparent agglomeration can be seen. By increasing the nanofiller content, multilayer stacks of GO are clearly evident in the image of uf-PLA/0.5GO, indicating lower efficiency of the applied flow field to disperse the nanoparticles at higher loadings.

3.3 | Viscoelastic responses of PLA sample incorporated with carbonaceous nanoparticles

The bubble nucleation and growth in the molten PLA occur after leaving the extrusion die, clarifying the significance of the rheological behavior of molten PLA. As shown in previous works,^{38–40} the more the improvement

in the viscoelastic behavior and melt strength, the more the enhancement in the foaming ability of polymers, particularly semi-crystalline polymers. Indeed, the addition of nanofillers influences the rheological behavior of PLA foams.⁴¹ Figure 5 demonstrates the storage and loss moduli along with complex viscosity versus angular frequency for different unfoamed samples. It can be observed that with the incorporation of the carbonaceous nanoparticles, the storage and loss moduli as well as complex viscosity (G' , G'' , and η^* , respectively) experience a slight decrement, and the sample containing 0.25 phr GO has the nearest rheological behavior to the neat sample. By adsorbing the polymer chains on the solid surface of nanoparticles, it is expected that PLA molecules entropy decreases, and chain relaxation time, τ_r , of PLA chains enhances.⁴² The mentioned influences can be studied with the investigation of the solid-like behavior and τ_r of the polymer chains in melt.⁴³ In the case of an un-reinforced linear homopolymer, G' and G'' are proportional to ω^2 and ω^1 , respectively, on the full logarithmic scale. This proportionality, especially at low-frequency region, is a liquid-like rheological behavior, which is also known as terminal behavior. However, a deviation from this proportionality, known as non-terminal behavior, was observed for a reinforced linear homopolymer. Deviation

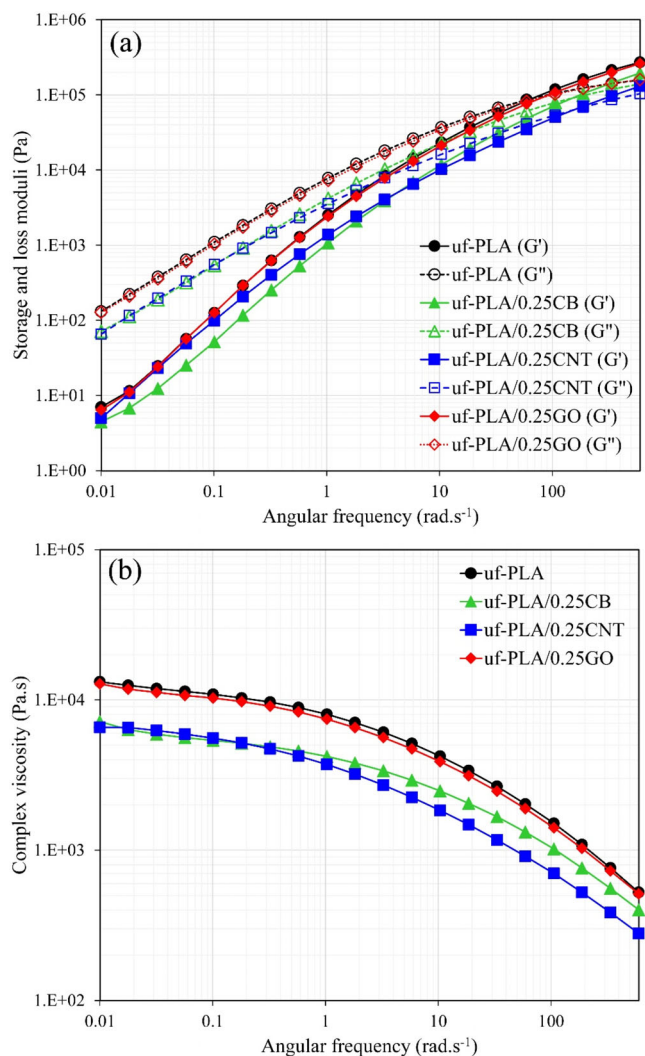


FIGURE 5 (a) Storage and loss moduli as well as (b) complex viscosity versus angular frequency measured at 170 °C and at 1% strain. [Color figure can be viewed at [wileyonlinelibrary.com](https://onlinelibrary.wiley.com/doi/10.1002/app.53823)]

from the mentioned relationship in filled polymeric systems is accompanied with the rheology of fluids with gel-like behavior. To put it another way, in the case of a reinforced polymer, G' and G'' are proportional to ω^a and ω^b , respectively, at the terminal region, where $a < 2$ and $b < 1$.^{44,45} The stronger the interactions between the polymer and the fillers and the significantly reduced the chain entropy, the more a and b tend to zero.⁴⁶ These exponents were calculated for the unfoamed PLA/CE sample and nanocomposites containing 0.25 phr of CB, CNT, and GO, and are listed in Table 2.

As seen, exponents a and b do not show noticeable changes with the addition of carbonaceous nanoparticles, among which incorporating 0.25 phr CB intensifies the non-terminal behavior to some extent. Thus, introducing carbonaceous nanoparticles does not considerably influence the rheological behavior of PLA melt. Similarly, the

longest relaxation time of chains (τ_{lr}) for all unfoamed samples is almost the same, and the sample loaded with 0.25 phr GO has the closest value to uf-PLA. The characteristic τ_{lr} can be achieved from the inverse of reciprocal crossover frequency (ω_r), in which G' and G'' are equal.^{43,45} It was expected that by adsorbing polymer chains on the nanofiller solid surfaces, τ_{lr} could be increased and the PLA melt viscoelastic characteristics would be improved, which play an important role in the bubble growth step.^{47,48} As a result, bubble wall rupture and gas removal occur less with the addition of nanofiller. However, in the extruded unfoamed samples, the expected enhancements in the viscoelastic characteristics of PLA melt were not observed. Overall, the presence of nanofillers can change the viscoelastic responses of PLA melt from two different viewpoints: first, nanoparticles improve the viscoelastic properties of PLA chains by absorbing the polymer chains on the nanofiller solid surfaces; second, nanofillers can increase the shear viscous heat of melt during melt-mixing in extruder channels, hence, intensifying the PLA chain scission reaction. It seems that the second influence of nanofillers slightly restricts the results of the first aforementioned effect.

The maximum temperature in the extruder temperature profile for the preparation of foam and unfoamed samples was 160 °C. At this low temperature, the used chain extender additive did not succeed in the ring-opening reaction of epoxy functional groups with the end-groups of PLA chains.⁴⁹ Therefore, the dominant reaction in the extrusion process of unfoamed samples is the unfavorable chain scission of PLA macromolecules. In the presence of nanofillers, the chain scission reactions of PLA is intensified owing to higher shear viscous heat and higher melt temperatures. Consequently, the presence of nanofillers causes more severe chain scission of PLA macromolecules. Without favorable CE reactivity, the lower molecular weight of PLA chains in uf-PLA nanocomposites worsens the rheological properties of the melt and this effect is stronger than the effect of restricted molecular motions of PLA in the presence of nanoparticles.

Nevertheless, in foam samples, the exothermic decomposition reaction of AzD foaming agent partially compensates the adverse effect of nanofillers.

3.4 | Effect of incorporating carbonaceous nanoparticles on the molecular weight alterations

Table 3 reveals the \overline{M}_n , \overline{M}_w , and PDI for the f-PLA foam and foams containing 0.25 phr of CB, CNT, and GO obtained from the GPC test. As seen, incorporating the

TABLE 2 Data related to the rheological behavior of unfoamed samples.

Sample code	$a(G' \propto \omega^a)$	$b(G'' \propto \omega^b)$	ω_r (1/s)	τ_r (s)
uf-PLA	1.274	0.916	67	15×10^{-3}
uf-PLA/0.25CB	1.074	0.879	153	7×10^{-3}
uf-PLA/0.25CNT	1.294	0.921	116	9×10^{-3}
uf-PLA/0.25GO	1.261	0.904	83	12×10^{-3}

TABLE 3 \overline{M}_n , \overline{M}_w , and PDI for different foamed samples achieved from the GPC test.

Sample code	\overline{M}_n (g/Mol)	\overline{M}_w (g/Mol)	PDI
f-PLA	1.33×10^4	8.31×10^4	6.27
f-PLA/0.25CB	1.36×10^4	8.76×10^4	6.45
f-PLA/0.25CNT	1.88×10^4	10.43×10^4	5.55
f-PLA/0.25GO	1.52×10^4	9.26×10^4	6.13

carbonaceous nanofillers into the PLA matrix increases the molecular weight of the matrix chains in the foam samples. Figure 6 shows schematically the reactions between the epoxy-based CE and the COOH end groups of PLA chains. By happening the chemical reactions displayed in Figure 6, the extrusion process can produce PLA macromolecules with longer branches and larger molecular weight. As a result, the content of larger molecular weight PLA chains increases. The epoxy groups of CE can theoretically react with both OH and COOH groups of PLA; however, COOH groups are more likely to react with electrophilic groups such as epoxide.⁵⁰ The work of Bikiaris and Karayannidis⁵¹ demonstrated that the epoxide groups on CEs react with the COOH end groups on PLA. It was also found that excess epoxide groups probably react with OH end groups and with the new OH groups originated from the linking of the epoxide and COOH groups. Comparing the nanocomposite foams with f-PLA reveals that adding 0.25 phr CB does not affect \overline{M}_n and \overline{M}_w . In contrast, the \overline{M}_n and \overline{M}_w of the foams reinforced with 0.25 phr CNT and 0.25 phr GO enhance than those of the pure PLA/CE foam, whereas their PDI experiences a little change. These outcomes reveal that carbonaceous nanoparticles, especially CNT and GO, intensify the CE reaction with PLA end groups and lead to more alterations in PLA molecular weight and structure. Although a fixed level of CE is applied in different nanocomposite foams and f-PLA sample, the chain extension effect of CE additive on PLA macromolecules depends on the nanofiller used. The beneficial structural changes of PLA chains in the presence of nanofillers improve the melt strength and foamability of matrix. As a result, the removal of gas from the decomposition reaction of the foaming agent is

prohibited, and foams having larger void contents are prepared by incorporating nanofillers.

The data of GPC analysis confirm that nanofillers, especially CNT and GO, can improve the chain extension reaction of CE additive comparing with f-PLA sample. It is noteworthy that the level of CE is fixed in f-PLA and nanocomposite foams. This improvement is in contrast to the nanofiller effects on the rheological properties of unfoamed samples. These opposite results originate from the temperatures at which the CE functional groups undergo the ring-opening reaction. As reported, the occurrence of this reaction is intensified at higher temperatures, especially above 200°C.⁴⁹ Because at the low temperature applied in the extrusion process, namely 140–160 °C, the reaction between CE and PLA chains cannot happen to a large extent in the compounding process of unfoamed samples. Therefore, the chain scission of PLA macromolecules is the dominant reaction in this process, and the higher melt temperature of PLA/nanofiller mixtures worsens the rheological behavior of PLA.

The heat generated by the decomposition reaction of AzD heightens the melt temperature in the extrusion foaming process, thus further activating the CE additive. Under these conditions, the presence of nanofillers, especially those with better dispersion and matrix/filler interfacial area, further increases the melt viscosity and generates more viscous heat. By rising the melt temperature, the chain extension reaction of CE becomes more extensive, hence improving PLA molecular weight, melt strength and foaming ability.

3.5 | Electrical conductivity

Figure 7 reveals the electrical conductivity of different foamed PLA samples versus different contents of carbonaceous nanoparticles. As observed, f-PLA demonstrated a very low electrical conductivity ($5.1 \text{ E-}14 \text{ S/m}$), indicating its high insulation characteristics. As expected, incorporating CB did not significantly influence the electrical conductivity of f-PLA, and it experienced a minor increase up to $5.43 \text{ E-}14 \text{ S/m}$ for f-PLA containing 1 phr CB. A similar result was seen in the work of Wu et al.,⁵²

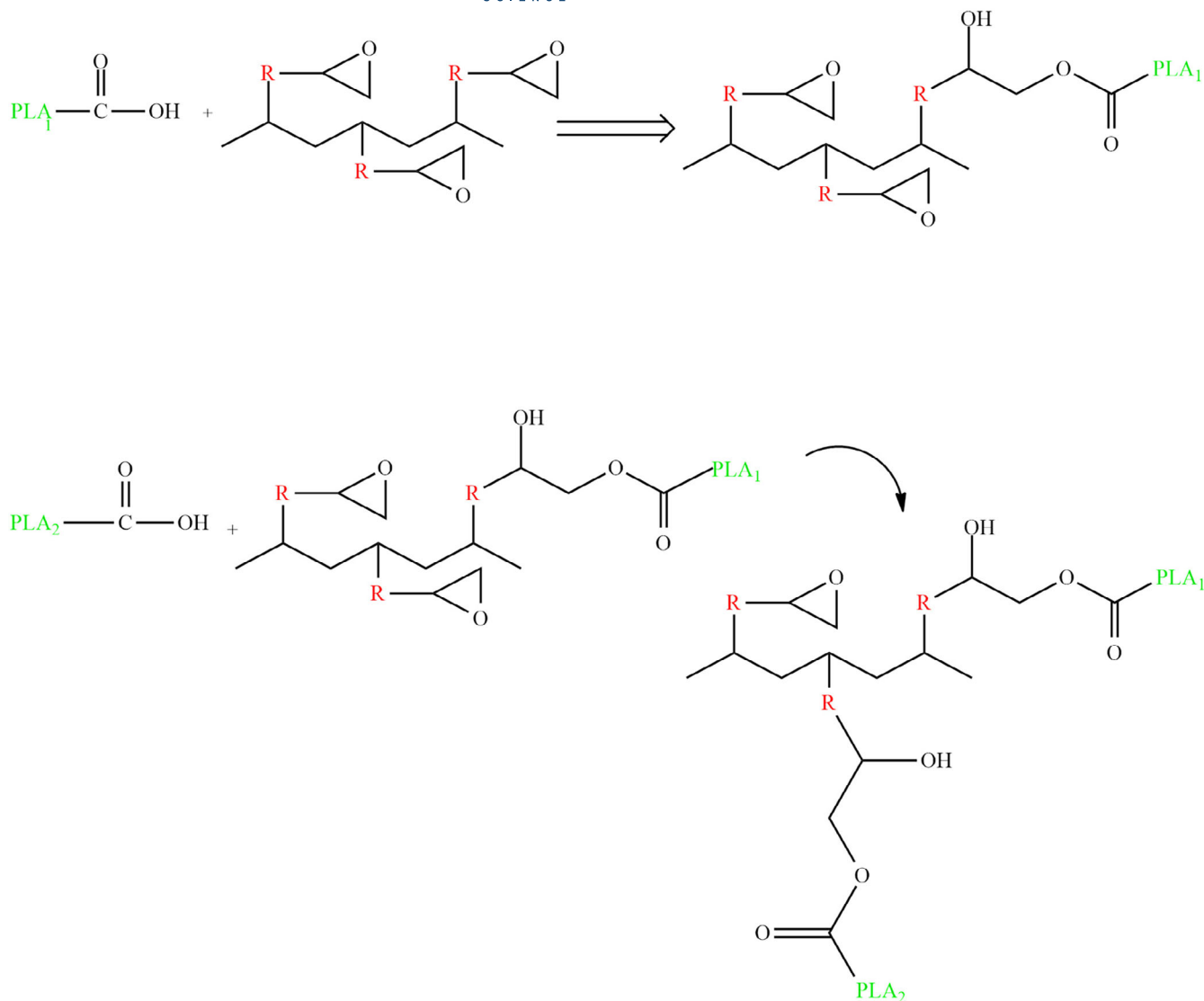


FIGURE 6 Schematic of the reaction between chain extender epoxy group and PLA end groups, and possible long chain branching structures. [Color figure can be viewed at [wileyonlinelibrary.com](https://onlinelibrary.wiley.com/doi/10.1002/app.53822)]

where adding CB up to 2 wt% did not remarkably affect the electrical conductivity of PLA foam. Adding different percentages of CNT and GO resulted in an improvement in the electrical conductivity of f-PLA. Specifically, the electrical conductivity of the foamed samples enhanced sharply by 9 and 10 orders of magnitude when the incorporation of CNT and GO, respectively, increased to 0.5 phr. These enhancements can be attributed to the high electrical conductivities of CNT and GO.⁵³ In addition, the electrical conductivities of the f-PLA/1CNT and f-PLA/1GO almost did not change compared to those of the samples containing 0.5 phr carbonaceous nanoparticles. This may be due to aggregation by adding 1 phr of nanofillers. It can also be seen that the electrical conductivity values for the foamed samples containing GO are higher than for CNT, approximately one order of magnitude, attributing to the higher electrical conductivity of GO compared to CNT.⁵³

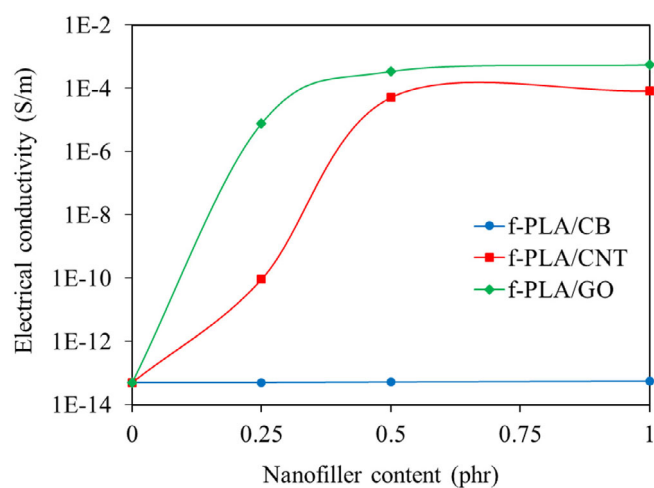


FIGURE 7 Electrical conductivity of different foamed PLA samples versus different percentages of carbonaceous nanoparticles. [Color figure can be viewed at [wileyonlinelibrary.com](https://onlinelibrary.wiley.com/doi/10.1002/app.53822)]

4 | CONCLUSIONS

In the present study, PLA foaming was performed using a twin-screw extrusion process. The foamability of PLA was improved by incorporating chain extender and carbonaceous nanofillers. The extruded f-PLA nanocomposites have enough melt strength and elasticity, so they will be able to provide foams with a density reduction of about 50%. These foams are lighter than virgin PLA and PLA/CE foam samples. The most optimum properties were seen in the foams filled with 0.25 phr CNT and 0.25 phr GO. The foam reinforced with 0.25 phr GO indicated the most increased void content ($\sim +45\%$) than virgin PLA foam, while its cell density experienced a diminishment by about 20%. In addition, although the foam filled with 0.25 phr CNT indicated a lower increment in the void content (+18%), its cell density was enhanced by 3% than the pure foam. Besides, the rheological behavior of all unfoamed PLA-based samples was almost the same, and the sample filled with 0.25 phr GO demonstrated the closest rheological behavior to the unfoamed PLA/CE sample. It was found from the gel permeation chromatography test results that the number- and weight-average molecular weights of the foams filled with 0.25 phr CNT and 0.25 phr GO enhanced than those of f-PLA foam. These results suggest that these carbonaceous nanofillers intensify the chain extender performance and result in beneficial structural changes in PLA chains. Comparing with CNT and GO, the addition of CB filler did not improve the foamability of PLA melt due to lower interfacial area with matrix at the same nanoparticle loadings. Moreover, the incorporation of different amounts of CB did not significantly change the electrical conductivity of virgin PLA foam, while the electrical conductivity of the foams containing 0.5 phr CNT and 0.5 phr GO enhanced sharply by 9 and 10 orders of magnitude, respectively. These improvements can be owing to the high electrical conductivities of CNT and GO. In addition, the electrical conductivities of the foams containing 1 phr CNT and 1 phr GO remained almost unchanged compared to those of the foams containing 0.5 phr CNT and 0.5 phr GO, attributing to the occurrence of aggregation after adding 1 phr CNT and GO.

AUTHOR CONTRIBUTIONS

Amirali Soleimanpour: Conceptualization (equal); data curation (equal); formal analysis (equal); investigation (equal); methodology (equal). **Hanieh Khonakdar:** Conceptualization (equal); data curation (equal); methodology (equal); resources (equal). **Seyed Rasoul Mousavi:** Resources (equal); visualization (equal); writing – original draft (equal). **Farkhondeh Hemmati:** Investigation (equal); supervision (equal); writing –

review and editing (equal). **Nastaran Banaei:** Data curation (equal); formal analysis (equal). **Mohammad Arjmand:** Validation (equal); writing – review and editing (equal). **Holger Ruckdäschel:** Project administration (equal); resources (equal). **Hossein Ali Khonakdar:** Project administration (equal); supervision (equal); writing – review and editing (equal).

ACKNOWLEDGMENT

Open Access funding enabled and organized by Projekt DEAL.

CONFLICT OF INTEREST STATEMENT

The authors declare that they have no conflict of interest.

DATA AVAILABILITY STATEMENT

The data that support the findings of this study are available from the corresponding author upon reasonable request.

ORCID

Holger Ruckdäschel  <https://orcid.org/0000-0001-5985-2628>

REFERENCES

- [1] S. R. Mousavi, S. Estaji, E. Rostami, H. A. Khonakdar, M. Arjmand, *Polym. Adv. Technol.* **2022**, *33*, 49.
- [2] S. Qewami, S. R. Mousavi, R. Ghanemi, J. Mohammadi-Roshandeh, H. A. Khonakdar, F. Hemmati, *Eur. Polym. J.* **2023**, *182*, 111729.
- [3] M. I. Tayouri, S. R. Mousavi, S. Estaji, S. Nemati Mahand, R. Jahanmardi, M. Arjmand, K. Arnhold, H. A. Khonakdar, *Polym. Adv. Technol.* **2022**, *33*, 2149.
- [4] M. R. Habibolah Zargar, S. R. Mousavi, A. Ebrahimzade, S. A. Mousavi Shoushtari, H. A. Khonakdar, *J. Elastomers Plast.* **2022**, *55*, 244.
- [5] S. Farjaminejad, S. Shojaei, V. Goodarzi, H. A. Khonakdar, M. Abdouss, *Eur. Polym. J.* **2021**, *159*, 110711.
- [6] A. Jafari, V. Fakhri, S. Kamrani, S. R. G. Anbaran, C.-H. Su, V. Goodarzi, V. Pirouzfard, H. A. Khonakdar, *Eur. Polym. J.* **2022**, *164*, 110984.
- [7] B. Ghassemi, S. Estaji, S. R. Mousavi, S. Nemati Mahand, S. Shojaei, M. Mostafaiyan, M. Arjmand, H. A. Khonakdar, *J. Mater. Sci.* **2022**, *57*, 7250.
- [8] M. Abrisham, M. Noroozi, M. Panahi-Sarmad, M. Arjmand, V. Goodarzi, Y. Shakeri, H. Golbaten-Mofrad, P. Dehghan, A. S. Sahzabi, M. Sadri, *Eur. Polym. J.* **2020**, *131*, 109701.
- [9] A. Paydayesh, S. R. Mousavi, S. Estaji, H. A. Khonakdar, M. A. Nozarinya, *Polym. Compos.* **2022**, *43*, 411.
- [10] S. R. Mousavi, M. H. Zamani, S. Estaji, M. I. Tayouri, M. Arjmand, S. H. Jafari, S. Nouranian, H. A. Khonakdar, *J. Mater. Sci.* **2022**, *57*, 3143.
- [11] R. Mokhtari Aghdami, S. R. Mousavi, S. Estaji, R. K. Dermen, H. A. Khonakdar, A. Shakeri, *Polym. Compos.* **2022**, *43*, 4165.
- [12] M. Arshian, S. Estaji, M. I. Tayouri, S. R. Mousavi, S. Shojaei, H. A. Khonakdar, *Polym. Adv. Technol.* **2023**, *34*, 985

- [13] A. Soleimanpour, H. Khonakdar, S. R. Mousavi, F. Hemmati, M. Arjmand, K. Arnhold, U. Reuter, H. A. Khonakdar, *Thermochim. Acta* **2022**, *716*, 179308.
- [14] F. Azadi, S. H. Jafari, H. A. Khonakdar, M. Arjmand, U. Wagenknecht, V. Altstädt, *Macromol. Mater. Eng.* **2021**, *306*, 2000576.
- [15] A. Jafari, H. Mirzaei, M. A. Shafiei, V. Fakhri, A. Yazdanbakhsh, V. Pirouzfard, C.-H. Su, S. R. Ghaffarian Anbaran, H. Khonakdar, *Polym. Adv. Technol.* **2022**, *33*, 1427.
- [16] A. Sharifi, S. R. Mousavi, R. Ghanemi, Z. Mohtaramzadeh, R. Asheghi, J. Mohammadi-Roshandeh, H. A. Khonakdar, F. Hemmati, *Int. J. Biol. Macromol.* **2023**, *233*, 123517.
- [17] W. J. Choi, K. S. Hwang, H. J. Kwon, C. Lee, C. H. Kim, T. H. Kim, S. W. Heo, J.-H. Kim, J.-Y. Lee, *Mater. Sci. Eng. C* **2020**, *110*, 110693.
- [18] H. Ding, W. Yang, W. Yu, T. Liu, H. Wang, P. Xu, L. Lin, P. Ma, *Compos. Commun.* **2021**, *25*, 100730.
- [19] H. Zhou, M. Zhao, Z. Qu, J. Mi, X. Wang, Y. Deng, *J. Polym. Environ.* **2018**, *26*, 3564.
- [20] Y. Li, H. Zhou, B. Wen, Y. Chen, X. Wang, *J. Polym. Environ.* **2020**, *28*, 17.
- [21] M. Nofar, A. Tabatabaei, H. Sojoudiasli, C. B. Park, P. J. Carreau, M.-C. Heuzey, M. R. Kamal, *Eur. Polym. J.* **2017**, *90*, 231.
- [22] J. M. Julien, J.-C. Quantin, J.-C. Bénézet, A. Bergeret, M. F. Lacrampe, P. Krawczak, *Eur. Polym. J.* **2015**, *67*, 40.
- [23] K. B. Venkatesan, S. S. Karkhanis, L. M. Matuana, *J. Appl. Polym. Sci.* **2021**, *138*, 50686.
- [24] A. Rostami, M. Vahdati, Y. Alimoradi, M. Karimi, H. Nazockdast, *Polymer (Guildford)* **2018**, *134*, 143.
- [25] S. Yang, Z.-H. Wu, W. Yang, M.-B. Yang, *Polym. Test.* **2008**, *27*, 957.
- [26] J. Rzayev, *Macromolecules* **2009**, *42*, 2135.
- [27] J. Ludwiczak, M. Kozłowski, *J. Polym. Environ.* **2015**, *23*, 137.
- [28] Q. Ren, J. Wang, W. Zhai, R. E. Lee, *Ind. Eng. Chem. Res.* **2016**, *55*, 12557.
- [29] Y. Liu, C.-L. Deng, J. Zhao, J.-S. Wang, L. Chen, Y.-Z. Wang, *Polym. Degrad. Stab.* **2011**, *96*, 363.
- [30] B. Palai, M. Biswal, S. Mohanty, S. K. Nayak, *Ind. Crops Prod.* **2019**, *141*, 111748.
- [31] M. Keshtkar, M. Nofar, C. B. Park, P. J. Carreau, *Polymer (Guildford)* **2014**, *55*, 4077.
- [32] Q. Guan, H. E. Naguib, *J. Polym. Environ.* **2014**, *22*, 119.
- [33] W. Liu, X. Zhu, H. Gao, X. Su, X. Wu, *Cell. Polym.* **2020**, *39*, 117.
- [34] S. Saeidlou, M. A. Huneault, H. Li, C. B. Park, *Prog. Polym. Sci.* **2012**, *37*, 1657.
- [35] Y. Li, D. Yin, W. Liu, H. Zhou, Y. Zhang, X. Wang, *Int. J. Biol. Macromol.* **2020**, *163*, 1175.
- [36] W. Wu, X. Cao, Y. Zhang, G. He, *J. Appl. Polym. Sci.* **2013**, *130*, 443.
- [37] S. M. H. Khademi, F. Hemmati, M. A. Aroon, *Int. J. Biol. Macromol.* **2020**, *157*, 470.
- [38] D. Eaves, *Handbook of polymer foams*, iSmithers Rapra Publishing, Shrewsbury, Shropshire **2004**.
- [39] E. Bahreini, S. F. Aghamiri, M. Wilhelm, M. Abbasi, *J. Cell. Plast.* **2018**, *54*, 515.
- [40] C. Zhao, L. H. Mark, S. Kim, E. Chang, C. B. Park, P. C. Lee, *Polym. Eng. Sci.* **2021**, *61*, 926.
- [41] G. Wang, G. Zhao, S. Wang, L. Zhang, C. B. Park, *J. Mater. Chem. C* **2018**, *6*, 6847.
- [42] F. Hemmati, O. Yousefzade, H. Garmabi, *Adv. Polym. Technol.* **2018**, *37*, 1345.
- [43] T. Nazari, H. Garmabi, A. Arefazar, *J. Appl. Polym. Sci.* **2012**, *126*, 1637.
- [44] C. G. Gogos, Z. Tadmor, *Principles of polymer processing*, John Wiley & Sons, Hoboken, New Jersey **2013**.
- [45] F. Hemmati, H. Garmabi, H. Modarress, *Polymer (Guildford)* **2014**, *55*, 6623.
- [46] K. A. Iyer, G. T. Schueneman, J. M. Torkelson, *Polymer (Guildford)* **2015**, *56*, 464.
- [47] M. Nofar, C. B. Park, *Prog. Polym. Sci.* **2014**, *39*, 1721.
- [48] W. Liu, X. Wang, H. Li, Z. Du, C. Zhang, *J. Cell. Plast.* **2013**, *49*, 535.
- [49] T. Standau, M. Nofar, D. Dörr, H. Ruckdäschel, V. Altstädt, *Polym. Rev.* **2022**, *62*, 296.
- [50] H. Inata, S. Matsumura, *J. Appl. Polym. Sci.* **1985**, *30*, 3325.
- [51] D. N. Bikiaris, G. P. Karayannidis, *J. Polym. Sci. A: Polym. Chem.* **1996**, *34*, 1337.
- [52] D. Wu, Q. Lv, S. Feng, J. Chen, Y. Chen, Y. Qiu, X. Yao, *Carbon N. Y.* **2015**, *95*, 380.
- [53] Y. Wang, G. J. Weng, *Micromechanics and Nanomechanics of Composite Solids*, Springer, **2018**, p. 123.

How to cite this article: A. Soleimanpour, H. Khonakdar, S. R. Mousavi, N. Banaei, F. Hemmati, M. Arjmand, H. Ruckdäschel, H. A. Khonakdar, *J. Appl. Polym. Sci.* **2023**, *140*(19), e53822. <https://doi.org/10.1002/app.53822>